



Development of low molecular weight heparin by H₂O₂/ascorbic acid with ultrasonic power and its anti-metastasis property

Xuemin Shen^a, Zhenfeng Liu^b, Junhui Li^a, Dongmei Wu^a, Meng Zhu^c, Lufeng Yan^a, Guizhu Mao^a, Xingqian Ye^a, Robert J. Linhardt^{d,*}, Shiguo Chen^{a,**}

^a Zhejiang Key Laboratory for Agro-Food Processing, Department of Food Science and Nutrition, Fuli Institute of Food Science, Zhejiang University, Hangzhou 310058, China

^b Institute of Health Products, Chiatai Qingchunbao Pharmaceutical Co., Ltd., Hangzhou 310023, China

^c Jiangsu Key Laboratory of Translational Research and Therapy for Neuro-Psycho-Diseases and College of Pharmaceutical Sciences, Soochow University, Suzhou, Jiangsu 215021, China

^d Center for Biotechnology & Interdisciplinary Studies, Department of Chemistry & Chemical Biology, Rensselaer Polytechnic Institute, Biotechnology Center 4005, Troy, NY 12180, USA

ARTICLE INFO

Article history:

Received 9 December 2018

Received in revised form 27 February 2019

Accepted 3 April 2019

Available online 04 April 2019

Keywords:

Low molecular weight heparin

Radical reaction

Ultrasonic degradation

Anti-metastasis

ABSTRACT

Low molecular weight heparins (LMWHs) are currently used as an anticoagulant agent since unfractionated heparin (UFH) can cause serious adverse drug reactions. LMWHs are commercially prepared using different methods such as nitrous acid cleavage and β -elimination under strong reaction conditions or with harsh chemicals, which may cause the saccharide units within the polysaccharide backbone to be decomposed and noticeably modified. This study demonstrates an effective method for depolymerizing heparin via the production of large amounts of free radicals from H₂O₂/ascorbic acid and ultrasonic power; this results in highly pure products because ascorbic acid can decompose during the reaction, which is different from the previously reported H₂O₂/Cu²⁺ method. The reaction conditions—including concentration of ascorbic acid, reaction temperature and intensity of ultrasonic power—were investigated and optimized. We found that the degradation behavior of heparin in this combined physicochemical process conformed to first-order reaction kinetics. The chemical composition and structures of different LMWHs were analyzed. The results showed the primary structure and sulfate esters were well preserved after the depolymerization, the major repeat units are (1–4)-linked glucosamine and iduronic acid. The further in vitro assays indicated that the LMWHs produced by H₂O₂/ascorbic acid with ultrasonic power have an anti-metastatic effect in A549 cells, which suggested the LMWHs rapidly prepared in this physicochemical way have a potential for anti-tumor metastatic function.

© 2019 Elsevier B.V. All rights reserved.

1. Introduction

Heparin is a complex acidic polysaccharide, which is characterized by a linear chain of a disaccharide unit of glucosamine bound to a hexuronic acid (including β -D-glucuronic acid and α -L-iduronic acid). The former includes 6-O-, 3-O-, N-sulfation and N-acetylation, and the latter can be 2-O-sulfation [1,2]. The average molecular weight of unfractionated heparin (UFH) is 15 kDa [3,4], which is widely used as a clinical anticoagulant that mainly inhibits the coagulation cascade by indirectly interacting with factor Xa and factor IIa (thrombin) for the prevention and treatment of thrombotic events [5]. However, heparins exhibit some undesirable side effects such as thrombocytopenia and

hemorrhagic complications [6,7]. In contrast, heparin substitutes—including low molecular weight heparin (LMWH, Mw~6 kDa) and ultra-low molecular weight heparin (ULMWH, Mw < 3 kDa)—that have a better bioavailability showed fewer side effects and have more predictable pharmacological activity and more sustained antithrombotic activity [8,9].

LMWHs are commercially available, such as enoxaparin, dalteparin, tinzaparin and parnaparin, among others. They are prepared through different processes, e.g. alkaline depolymerization [10] is carried out by direct treatment of heparin with NaOH under certain conditions. Oxidative depolymerization [11] uses various reagents like hydrogen peroxide or ionizing gamma radiation to break heparin down oxidatively. Enzymatic depolymerization of heparin is carried out by using heparinase I to cleave heparin into LMWH by β -elimination [12,13]. Deaminative degradation of heparin uses nitrous acid or isoamyl nitrite [10]. Photochemical degradation of unfractionated heparin [14] begins with photolysis using TiO₂ in distilled water. The methods mentioned above which use enzymes are costly, and the chemical methods require

* Correspondence to: R.J. Linhardt, Department of Chemistry & Chemical Biology, Rensselaer Polytechnic Institute, Biotechnology Center 4005, Troy, NY 12180, USA.

** Correspondence to: S. Chen, College of Biosystem Engineering and Food Science, Zhejiang University, Hangzhou 310029, China.

E-mail addresses: Linhar@rpi.edu (R.J. Linhardt), chenshiguo210@163.com (S. Chen).

strong reactions accompanied by many side reactions that reduce the efficiency of the final product. Therefore, a safe, costless and efficient method for producing LMWHs is needed.

Ultrasonic depolymerization has been used for years in different polysaccharides such as chitosan, starch [15], polysaccharide from a Red Algae [16] and curdlan [17], which demonstrated that degradation is caused both by OH radicals and mechanochemical effects at the applied ultrasound frequency. Furthermore, depolymerization of polysaccharides using ultrasound combined with other chemical reactions has received great attention in recent years. The ultrasonic-assisted degradation, comprised of the use of hydrogen peroxide-catalyzed radical hydrolysis and ultrasonic power—because of its strong penetrating power—has been used in various polysaccharides like chitosan [18], cellulose [19], glycosaminoglycan from sea cucumber [20] and fucosylated chondroitin sulfate [21]. The free radicals generated by metallic catalysts like copper (II) promote the degradation of polysaccharide when coupled with hydrogen peroxide, but this causes some unexpected results, such as the decrease of pH and the difficulty in removing the metallic catalysts after depolymerization [21,22]. In contrast, the method utilizing free radicals generated by ascorbic acid with H₂O₂ in this study is more effective, green and convenient.

In the present study, we applied a physicochemical method involving H₂O₂/ascorbic acid-assisted ultrasonic power to produce LMWHs. The influence of the reaction parameters—such as the concentration of ascorbic acid, reaction temperature, and ultrasound power on the decrease of molecular weight and degradation kinetics of UFH were investigated and optimized. The molecular weight and chemical compositions of LMWHs were also determined, and their primary structures were analyzed and compared by Fourier Transform infrared spectroscopy (FT-IR) and nuclear magnetic resonance (NMR). Furthermore, the anti-metastasis effect of UFH and its degraded products were investigated. The current investigation may provide an efficient and environmentally friendly method for producing low molecular weight sulfated polysaccharides.

2. Material and methods

2.1. Materials

The heparin was purchased from OURCHEM (Shanghai, China). Gel-filtration column Ultrahydrogel 250 was from Waters. Hydrogen peroxide, ascorbic acid, HPLC-grade methyl alcohol and deuterium oxide were obtained from Sinopharm Chemical Reagent Co., Ltd. (Shanghai, China). Heparinase I, II and III were obtained from Adhoc International Technologies Co., Ltd. (Beijing, China). Other chemical reagents were acquired from Aladdin Chemical Reagent Co., Ltd. (Shanghai, China). A549 cells were kindly donated by the Zhejiang Academy of Medical Sciences.

2.2. Physicochemical depolymerization of heparin: ultrasonic-assisted radical depolymerization

Heparin was dissolved in 0.1 M NaAc buffer (pH 6.8) to a final concentration of 5 mg/mL, mixed with ascorbic acid dissolved in 0.1 M NaAc, total volume of the above solution was 20 mL, then H₂O₂ at a concentration of 40 mM was added. Ultrasound treatments were performed (Scientz-IIID, Ningbo Scientz Biotechnology Co., Ningbo, China) with the following parameters: maximum ultrasound power output, 950 W; frequency, 22 kHz; intermittent type, 2 s on and 2 s off; and horn micro tip diameter, 10 mm. The samples were placed in a cylindrical glass reactor (Φ, 2.90 cm) and the generator probe was submerged about 1 cm below the liquid's surface to release ultrasonic energy. The whole reaction time was 50 min; during the process, we took 100 μL degraded samples every 10 min and adjusted them to a pH of 10–11 with 1 M NaOH in order to stop the reaction. Reaction conditions—including concentration of ascorbic acid (1, 5, 10, 20, 30 mM), reaction temperature (0, 15, 25, 35 and 45 °C) and ultrasound intensity (4.0, 7.1, 11.9,

16.6 and 21.4 W/mL)—were optimized. The dried heparin samples were collected for further gel permeation chromatography (GPC). After that, UFH and three low molecular weight samples with different degrees of depolymerization were collected for further disaccharide analysis, FTIR, NMR, cell viability and scratch wound assays. Three samples with different degree of depolymerization obtained under 40 mM H₂O₂, 16.6 W/mL ultrasound intensity, pH 6.8 and 25 °C with 1 mM, 30 mM and 10 mM ascorbic acid were named after LMWH-1, LMWH-2, LMWH-3, respectively.

2.3. GPC-HPLC analysis

The change in molecular weight of the degraded heparin samples was determined by GPC according to our previous studies, with a few additional modifications. The GPC was performed on a Waters Ultrahydrogel 250 column (3.9 × 300 mm) (Milford, MA, USA) at 40 °C and eluted using 0.2 M NaCl aqueous solution at a flow rate 0.5 mL/min monitored with a refractive index detector. Sulfated oligosaccharide standards [23] from our group were used to determine the molecular weight of the samples.

2.4. Analysis of heparin disaccharide by SAX-HPLC

The mixture of heparinase I, II and III (0.5 IU/mL, 100 μL of each heparinase) were added to UFH and LMWH samples (100 μL of a 5 mg/mL solution in water) and incubated at 37 °C for 48 h. The heparinase I, II and III were dissolved in potassium phosphate buffer (pH 7.0, 10 mM KH₂PO₄ and 0.2 mg/mL of bovine serum albumin) beforehand.

The exhaustively-digested heparin (3 μL) was injected onto a Waters Spherisorb SAX column (250 × 4.0 mm, 5 μm). The analysis was performed on an Agilent 1260 system equipped with dual pumps (Agilent, CA, USA). Mobile phase A was 2.64 mM NaH₂PO₄ at a pH of 3.0 and mobile phase B was an aqueous solution of 2.64 mM NaH₂PO₄ with 1.14 M NaClO₄ at a pH of 3.0. The linear gradient of mobile phase B was 3%–35% B (0–20 min), 35%–100% B (20–50 min), 100% B (50–55 min) with a flow rate of 0.6 mL/min. The column temperature was 40 °C. UV 232 nm was selected as the detection.

2.5. Kinetics models of degradation

Our process of free radical depolymerization of heparin followed first-order reaction kinetics. The degradation rate constant (*k'*) was determined as the following equation:

$$1/M_w(t) - 1/M_w(0) = k' t$$

In this equation, *M_w*(0) was the initial molecular weight; and *M_w*(*t*) was during free radical degradation at *t* minutes. Meanwhile, *k'* (mol · g⁻¹ · min⁻¹) was the first-order rate constant for change of weight average molecular weight.

2.6. Structural analysis by FTIR

For IR spectroscopy, samples of approximately 3 mg were ground together with 200 mg KBr and were analyzed by FTIR spectrum measurement in the frequency range of 4000–400 cm⁻¹ with 32 scans and a 4 cm⁻¹ resolution. The FTIR spectrum was taken on a Nicolet Avatar 370 instrument.

2.7. Nuclear magnetic resonance analysis of degradation products

¹H NMR of UFH and LMWHs and 2D NMR of LMWH-3 were performed by using a 600 MHz NMR spectrometer (DD2-600; Agilent Technologies Inc., CA, US) at 25 °C. The samples (10 mg) were vacuum frozen with 500 μL D₂O (99.96%) twice, followed by dissolution

in 500 μL D_2O . The samples were acquired in D_2O with chemical shifts expressed as δ PPM, using the resonances of CH_3 groups of acetone (δ 30.2/2.22) as an internal reference. The spectra were processed using the MestReNova 6.1.1 (Mestrelab Research, Santiago de Compostela, Spain).

2.8. Anti-metastatic property of LMWHs

2.8.1. Cell viability assay

The effect of UFH and LMWHs on the cell viability of A549 cells was evaluated by using the MTT assay [24] with a slight adjustment. Briefly, the cells were incubated in Rosewell Park Memorial Institute (RPMI)-1640 and supplemented with 10% fetal bovine serum (FBS), 100 U/mL of penicillin and 100 g/mL of streptomycin at 37 °C in a humidified incubator at 5% CO_2 . One hundred μL of the cells were incubated in a 96-well plate at a concentration of 2×10^5 cells/mL. After 24 h of cultivation at 37 °C, various concentrations of UFH and LMWHs (30, 60, 125, 250, and 500 $\mu\text{g}/\text{mL}$) were added slowly into the 96-well plate and cultured for 48 h. At the end of each treatment, 20 μL of MTT (5 mg/mL) were added, and the tumor cells were further incubated for 4 h for the formation of the formazan crystals. A volume of 100 μL of dimethyl sulfoxide (DMSO) was added to each well to dissolve the formazan crystals after the medium was removed. Subsequently, absorbance was measured at 490 nm with a microplate reader (Thermo multiscan Mk3, Thermo Fisher Scientific Inc., USA). The cell viability was expressed as:

$$\text{Cell viability (\%control)} = [(A_s - A_b)/(A_c - A_b)] \times 100$$

A_c and A_b were the absorbance of the system without the addition of polysaccharides and cells, respectively; A_s was the absorbance of the system with only polysaccharides.

2.8.2. The scratch wound assay

The wound healing assay was used to evaluate cell migration [25]. Briefly, A549 cells were cultured in 6-well plate (0.5×10^6 cells/well) at 37 °C for 24 h. A straight scratch was made with a 200 μL pipette tip on to simulate a wound, and the cell debris was removed, and the edge of the scratch was smoothed by washing with the growth medium. The wound was exposed to UFH and LMWHs at the concentration of 250 $\mu\text{g}/\text{mL}$, and 500 $\mu\text{g}/\text{mL}$, which were added to the wells and incubated for 24 h and 48 h at 37 °C. The cells without treatments were used as controls. The closure of the scratch was photographed under a phase contrast inverted microscope (AM IL LED, Leica, Germany). The scratch area was measured using ImageJ software (National Institutes of Health, Bethesda, MD, USA), and the percentage of the wound healing was calculated. Statistical analysis was performed by IBM SPSS 20.0 software.

3. Results and discussion

3.1. Effects of reaction parameters on heparin degradation

Radical-catalyzed hydrolysis was combined with ultrasonic waves to degrade the heparin in a highly efficient manner. The effects of the reaction parameters—including the concentration of ascorbic acid, reaction temperature and ultrasound power—were investigated in the present study during the depolymerization process on the degradation efficiency to optimize the depolymerization conditions. From GPC-HPLC spectrum (Fig. 1), the molecular weight of heparins decreased as the depolymerization deepens. The kinetic rate constant k' and the coefficient of determination in the equation (R^2) are shown in Table 1.

A neutral initial pH (NaAc buffer, pH 6.8) is required for an optimized degradation to prevent the acidic or basic hydrolysis of the heparin. Generally, the molecular weight of heparin was sharply reduced in the first 10 min and then more slowly reduced over the next 40 min

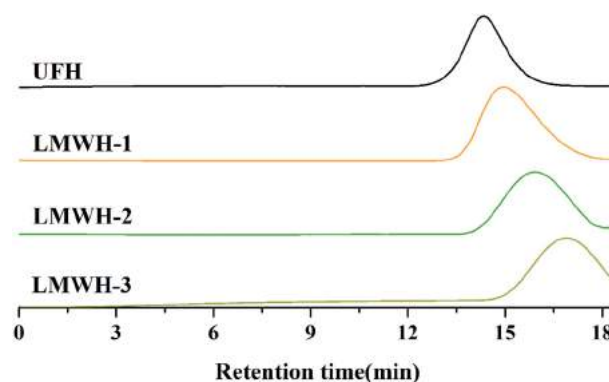


Fig. 1. GPC-HPLC spectrum of the UFH and degradation samples.

(Fig. 2). The average molecular weight was approximately equal to 2 kDa under the optimum reaction conditions, deeper degradation occurred, better than the previous studies [26] that described how the combination of hydrogen peroxide with ultrasonic waves enhanced the efficacy of depolymerization. The factors affecting the degradation of heparin were discussed as follows.

3.1.1. Effects of ascorbic acid concentration on the degradation efficiency

The amount of free radical generated from the H_2O_2 in the solution increased with the concentration of ascorbic acid increasing, which can also result in a significant decrease in the molecular weight of the depolymerized products (Fig. 2a). The increasing concentration of ascorbic acid from 1 mM to 10 mM could obviously elevate the degradation efficiency, while increasing the concentration of ascorbic acid from 10 mM to 30 mM had the opposite effect, judged by the change in the kinetic rate constant (Fig. 2b). The values of the kinetic rate constant k' increased when the concentration of ascorbic acid increased from 1 mM to 10 mM. At low concentrations, ascorbic acid is generally prone to be a pro-oxidant; at high concentrations, it will tend to be an antioxidant [27]. Hence, there is a crossover effect. When the amount of H_2O_2 was certain, the dehydrogenated form (Eqs. (1) and (2)) auto-oxidized by the extra ascorbic acid was likely to react with hydroxyl radicals generated from the H_2O_2 /ascorbic acid redox system (Eq. (3)) [28], resulting in a decrease of degradation efficiency. Based on these results, 10 mM was the optimal concentration of ascorbic acid in the solution because the optimized proportion to the concentration of H_2O_2 was 1:4.



Table 1

Degradation rate coefficients k' and the coefficient of determination from Eq. (1) R^2 for heparin degradation.

Process		k' ($\text{mol} \cdot \text{g}^{-1} \cdot \text{min}^{-1}$)	R^2
Ascorbic acid concentration (mM)	1	2.247×10^{-6}	0.967
	5	5.353×10^{-6}	0.952
	10	8.736×10^{-6}	0.974
	20	8.257×10^{-6}	0.991
	30	3.356×10^{-6}	0.959
Temperature (°C)	0	1.827×10^{-6}	0.940
	15	2.376×10^{-6}	0.959
	25	8.736×10^{-6}	0.974
	35	5.281×10^{-6}	0.961
	45	3.505×10^{-6}	0.953
Ultrasound intensity (W/mL)	4	2.467×10^{-6}	0.975
	7.1	2.705×10^{-6}	0.976
	11.9	4.716×10^{-6}	0.960
	16.6	8.736×10^{-6}	0.974
	21.4	3.137×10^{-6}	0.967

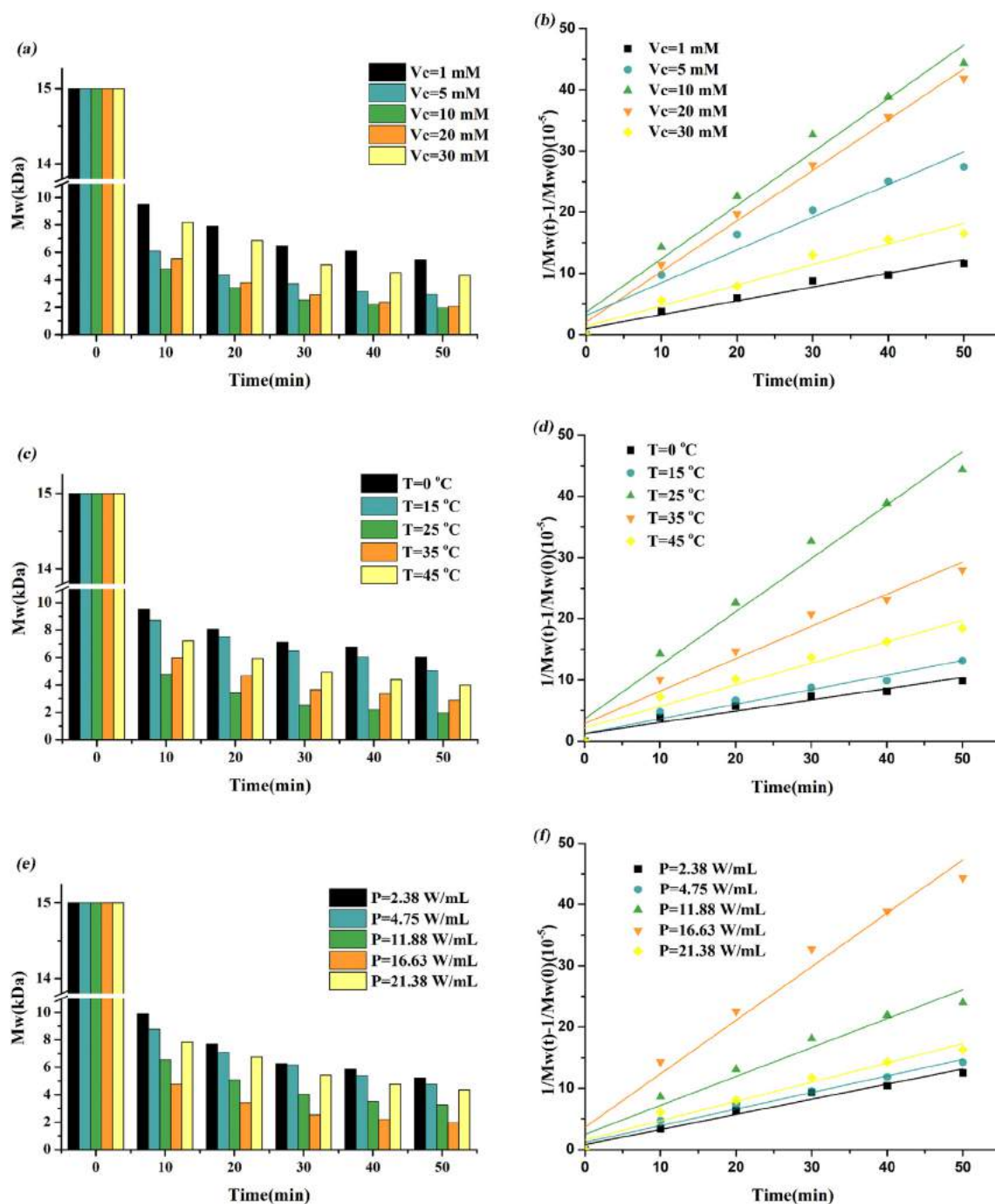
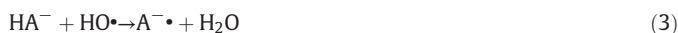


Fig. 2. Effect of different reaction conditions on the molecular weights of degraded heparin and its kinetics degradation: (a) Different ascorbic acid concentrations (1, 5, 10, 20 and 30 mM; H_2O_2 concentration, 40 mM; reaction temperature, 25 °C; ultrasound intensity, 16.63 W/mL); (b) Kinetics of heparin degradation at different ascorbic acid concentrations; (c) Different reaction temperatures (0, 15, 25, 35, 45 °C; H_2O_2 concentration, 40 mM; ascorbic acid concentration, 10 mM; ultrasound intensity, 16.63 W/mL); (d) Kinetics of heparin degradation at different reaction temperatures; (e) Different ultrasound intensities (2.38, 4.75, 11.88, 16.63, and 21.38 W/mL; H_2O_2 concentration, 40 mM; ascorbic acid concentration, 10 mM; reaction temperature, 25 °C); (f) Kinetics of heparin degradation at different ultrasound intensities.



3.1.2. Effects of reaction temperature on the degradation efficiency

The effects of temperature on UFH degradation is shown in Fig. 2c and Fig. 2d. Temperature can affect chemical and physical properties in different manners. On one side, high temperature helps to break the chemical bonds between monomer units and generates free radical

fragments, but high temperature also leads to a cushioned collapse [29]. We can see (Fig. 2c) the average molecule weight of the degradation production decreased when the temperature was increased from 0 °C to 25 °C; no obvious improvement in depolymerization efficiency was observed as temperature increased from 25 °C to 45 °C. At high temperatures, ascorbic acid and H_2O_2 may start to decompose, resulting in the decrease of free radical generation. Shown in Fig. 2d, the maximum value of the kinetic rate constant was found when the temperature was 25 °C compared to the other four reaction temperatures. Thus, 25 °C was selected as the optimal reaction temperature.

3.1.3. Effects of ultrasonic power on the degradation efficiency

As is shown in Fig. 2e, the average molecular weight decreased from 15 to 5.2, 4.8, 3.3, 2.1, and 4.3 kDa under ultrasonic intensities of 2.38, 4.75, 11.88, 16.63 and 21.38 W/mL, respectively, in 50 min. Because of its cavitation effects, ultrasound can significantly enhance the degradation of the heparin. Ultrasound waves are known to cause ruptures in the liquid phase in the form of small bubbles (cavities) filled with vapor, and some cavities violently collapse and induce high pressure gradients and high local velocities of the liquid layers in their vicinity [26]. In a certain range, higher ultrasonic power could increase the energy of cavitation and enhance the quality of the cavitation bubbles. From Fig. 2f we can see the degradation efficiency from the k' value was markedly higher under the power intensity of 16.63 W/mL. At higher intensities of sound waves, however, there was a large number of gas bubbles in the solution which scattered the sound waves to the walls of the vessel or back to the transducer. Thus, lesser energy is dissipated in the liquid from cavity formation, even when the vessel is exposed to higher and higher intensities [30].

Based on the results we obtained, we decided the values of 25 °C reaction temperature, 10 mM concentration of ascorbic acid and 16.63 W/mL ultrasound intensity were our optimal reaction conditions for depolymerization of UFH in highest efficiency among these reaction conditions. The combination of the H_2O_2 /ascorbic acid redox system with ultrasonic waves was used to generate hydroxyl radicals in high efficiency, which is also more environmentally friendly than combining use of copper (II) and H_2O_2 with ultrasound to generate hydroxyl radicals.

3.2. Disaccharide analysis

Low molecular products of heparin and UFH (before depolymerization) were prepared for further investigation of structure characterization and anti-metastasis property. Three samples with different degree of depolymerization obtained under 40 mM H_2O_2 , 16.6 W/mL ultrasound intensity, pH 6.8 and 25 °C with 1 mM, 30 mM and 10 mM ascorbic acid were named after LMWH-1 (6.9 kDa), LMWH-2 (4.3 kDa), LMWH-3 (2.1 kDa), respectively.

Disaccharide analysis is the basis for exploring the structure change, eight heparin disaccharides were separated under optimized conditions, and their proportions were shown in Fig. 3. As a whole, the content of eight different disaccharides in these polysaccharides was ranged from high to low as $\Delta IS > \Delta IIS > \Delta IIIS > \Delta IIA > \Delta IVA > \Delta IA > \Delta IVS > \Delta IIIA$, which indicated there are no major changes in the

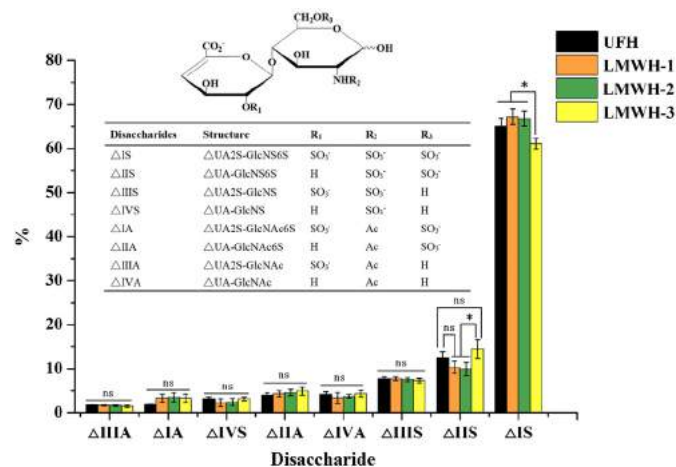


Fig. 3. Structures of heparin disaccharide standards and the percentage of each disaccharide in eight disaccharides. (mean \pm SD, $n = 3$, * represents $p < 0.05$, ns means no significant difference).

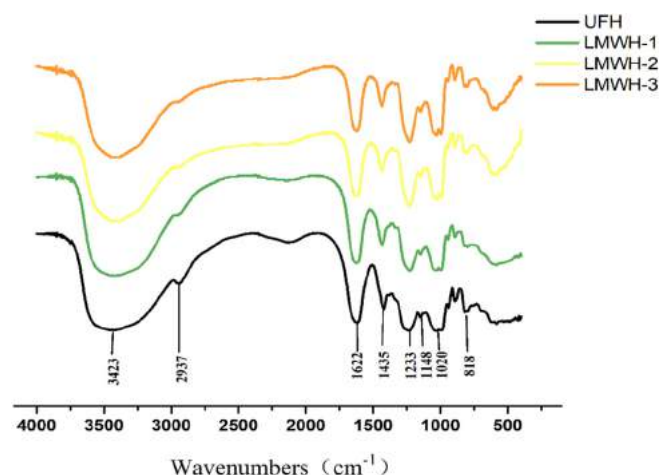


Fig. 4. IR spectra of UFH and LMWHs prepared by ultrasound/ H_2O_2 /ascorbic acid process. LMWH-1, LMWH-2 and LMWH-3 were prepared by US/ H_2O_2 /ascorbic acid system to 6.9 kDa, 4.3 kDa and 2.1 kDa.

disaccharide composition of UFH and three different degraded samples. The major disaccharide unit is 2-O-sulfated uronic acid and 6-O, N-sulfated glucosamine, whose proportion was approximately 60–70%. As the degradation deepens and the molecular weight decreases, there was a slight increase in $\Delta UA-GlcNS6S$ content in LMWH-3, presumably resulting from the loss of sulfa groups in $\Delta UA2S-GlcNS6S$. These minor changes corresponding to desulfonation for di- and trisulfated disaccharide because the sulfa groups are relatively unstable [31], thus the produced hydroxyl radicals were more likely to selectively attack certain sites within heparin.

3.3. FTIR spectrum

The FTIR spectra of UFH and low molecular weight products were examined and compared to show the precise changes in primary groups and sulfated parts. The FTIR spectra of heparin before and after being depolymerized are shown in Fig. 4. Both UFH and its depolymerized products display similar spectral bands. The broad peak centered at around 3423 cm^{-1} , assigned to the stretching vibration of $-OH$, became to be narrower as the decrease of molecular weight of heparin. A peak related to the stretching vibration of $C-H$ bonds was seen at 2937 cm^{-1} . These two major absorption peaks were commonly observed in polysaccharides [32]. Two peaks at 1622 cm^{-1} and 1435 cm^{-1} were attributed to bending vibration of amido groups ($-NH_2$) and the symmetric stretching of $-NO_2$, the intensity of the former decreased while the latter increased, which indicated that the amino groups of heparin might oxidize with hydroxyl radicals. The absorbance at 1233 cm^{-1} and 1020 cm^{-1} is due to $-SO_3^-$ asymmetric and symmetric stretching, respectively. Both their intensities were slightly increased after treatment, indicating that hydroxyl radicals might act in these sites. And between the above two peaks, the absorbance at 1148 cm^{-1} is due to asymmetric stretching of $C-O-S$. The bands observed in the $797-818\text{ cm}^{-1}$ are related to sulphate half esters' absorptions [33,34].

3.4. NMR spectra analysis

The 1H NMR spectra of UFH and LMWHs were obtained to better understand the structural change of heparin after depolymerization in Fig. 5. Generally, the depolymerized heparins exhibited similar spectra and contained similar characteristic signals to UFH, which indicated the H_2O_2 /ascorbic acid system assisted with ultrasonic treatment did

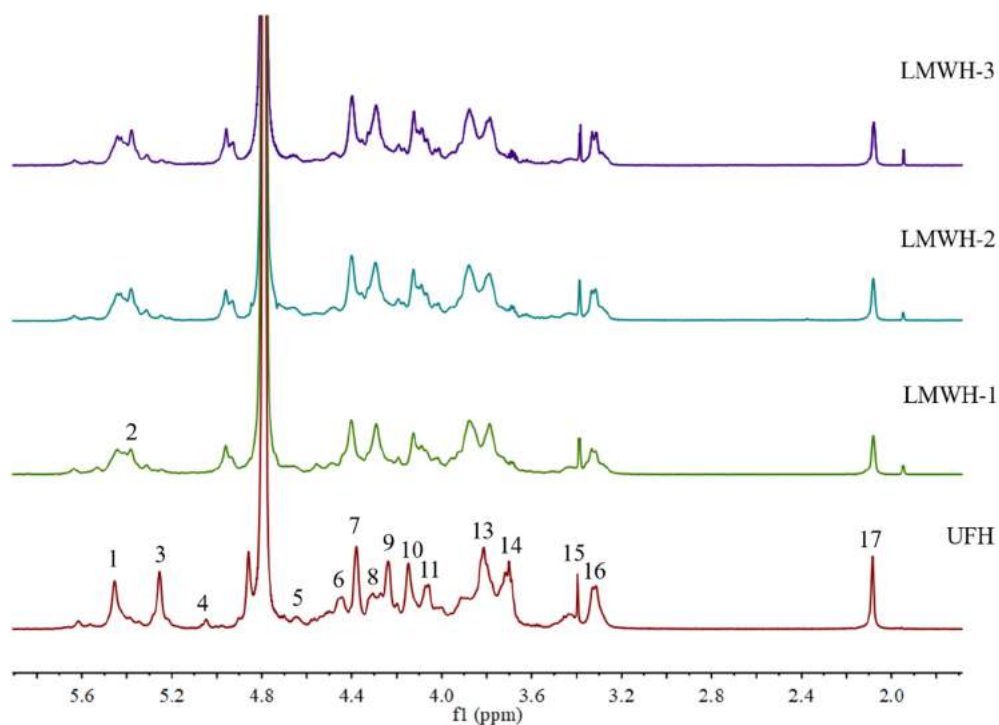


Fig. 5. ^1H NMR spectra of UFH and LMWHs prepared by ultrasound/ H_2O_2 /ascorbic acid process. LMWH-1, LMWH-2 and LMWH-3 were prepared by US/ H_2O_2 /ascorbic acid system to 6.9 kDa, 4.3 kDa and 2.1 kDa. (1, H1 GlcNS6S; 2, H1 GlcNS (linked IdoA2S); 3, H1 IdoA2S; 4, H5 IdoA2S; 5, H1 GlcA; 6, H6a GlcNS6S; 7, H2 IdoA2S; 8, H6b GlcNS6S; 9, H3 IdoA2S; 10, H4 IdoA2S; 11, H5 GlcNS6S; 12, H6 GlcNS; 13, H4 GlcNS6S; 14, H3 GlcNS; 15, H2 IdoA; 16, H2 GlcNS6S; 17, N-COCH₃, GlcNAc).

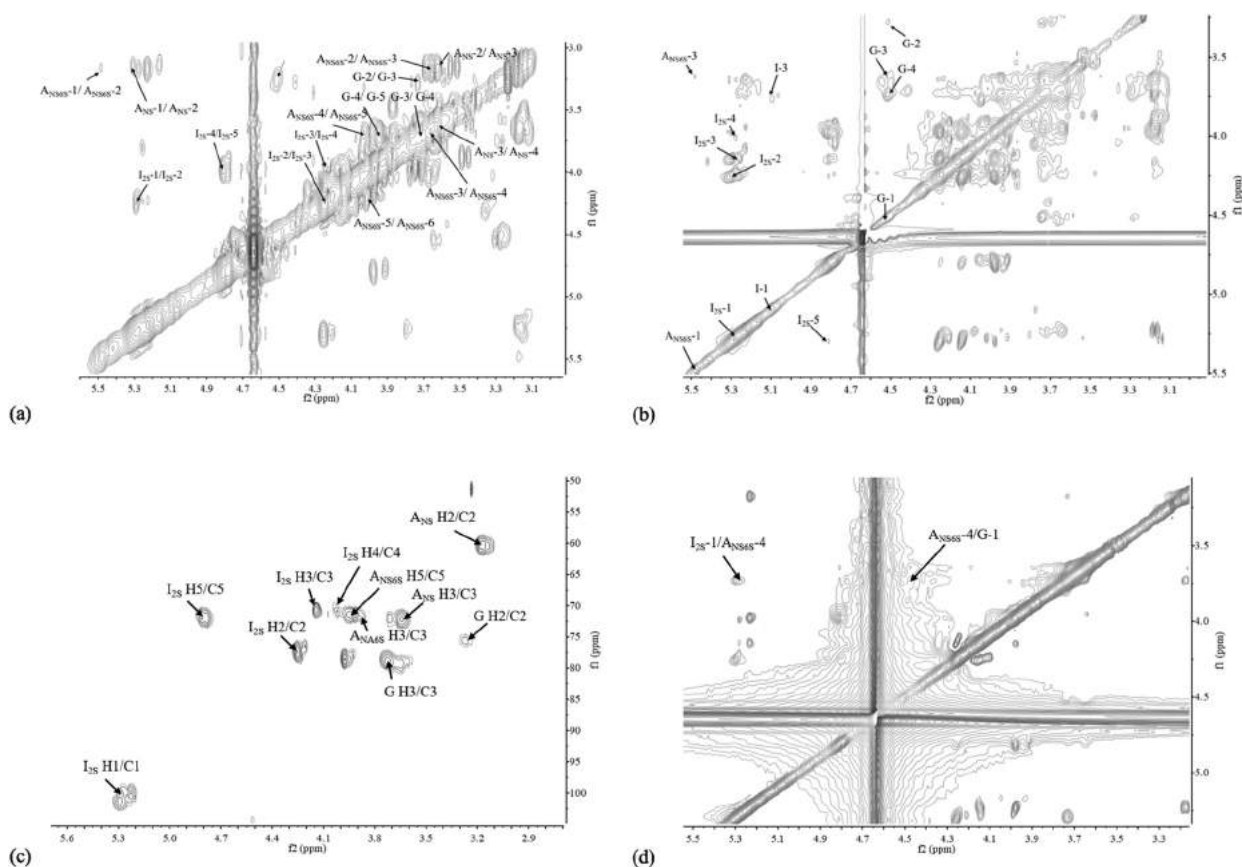


Fig. 6. 2D NMR spectra of LMWH-3 (a) COSY of LMWH-3; (b) TOCSY of LMWH-3; (c) HSQC of LMWH-3; (d) ROESY of LMWH-3. LMWH-3 was prepared by ultrasound/ H_2O_2 /ascorbic acid process (ascorbic acid concentration, 10 mM; reaction temperature, 25 °C; ultrasound intensity, 16.63 W/mL).

Table 2
¹H/¹³C NMR chemical shifts assignments of LMWH-3.

	GlcNS6S	GlcNS	IdoA2S	GlcA	IdoA	GlcNAc
H-1 (C-1)	5.48	5.31	5.28 (101.36)	4.49	5.10	
H-2 (C-2)	3.16	3.17 (60.31)	4.24 (77.48)	3.28 (75.67)	3.39	
H-3 (C-3)	3.62	3.66 (72.14)	4.13 (70.60)	3.63 (78.80)	3.76	
H-4 (C-4)	3.76	3.67	4.02 (70.86)	3.74	3.70	
H-5 (C-5)	4.02 (71.39)		4.81 (71.76)			
H-6 (C-6)	4.43/4.20	3.91				
–CH ₃						2.08

not change the fundamental structure of heparin. There were more signal peaks in the degraded LMWHs as the decrease of molecular weight compared to UFH, because of the interaction force between the sugar rings were weakening during the progress of depolymerization. The main peaks were assigned as follows: in the anomeric region, the signals at 5.46 ppm, 5.38 ppm and 5.25 ppm were assigned to H-1 of GlcNS6S, GlcNS, and IdoA2S, respectively. Then we can see the main peak signals at 4.37 ppm, 4.24 ppm and 4.15 ppm were assigned to the H-2, H-3 and H-4 of IdoA2S. And the signals at 4.43 ppm, 4.31 ppm, 4.06 ppm and 3.31 ppm were assigned to GlcNS6S. The disappearance or weakening of the signals observed at 5.25 ppm and 4.06 ppm suggests a partial desulfurization of uronic acid and glucosamine during the depolymerization of UFH. Moreover, the signal at 2.08 ppm represents the methyl protons of GalNAc (COCH₃). These results suggest that depolymerization of heparin by H₂O₂/ascorbic acid and ultrasonic power was achieved without compromising the core structure. The 2D NMR of LMWH-3, such as correlation spectroscopy (COSY, Fig. 6(a)), total correlation spectroscopy (TOCSY, Fig. 6(b)), heteronuclear single quantum coherence (HSQC, Fig. 6(c)) spectra and rotating frame overhauser enhancement spectroscopy (ROESY, Fig. 6(d)), were used to further assign the ¹H and ¹³C chemical shifts of the main parts of LMWH-3 due to the limited resolution of the ¹H NMR spectra. While the LMWH-3 is a heparin mixture, it is not possible to assign all of the signals in NMR spectra. Some assignments of ¹H and ¹³C chemicals shifts of LMWH-3 are shown in Table 2. The correlation peaks of H1 (IdoA2S)/H4 (GlcNS6S) at 5.28/3.76 ppm in ROESY spectra indicated that these two units are linked by the 1–4 position, which was consistent with the results we see from disaccharide analysis that ΔUA2S–GlcNS6S are the major parts.

3.5. Anti-metastasis of LMWHs

3.5.1. Cell viability assay

The cell viability of A549 cells treated with UFH and LMWHs at different concentrations (30, 60, 125, 250, and 500 μg/mL) using the MTT assay is shown in Fig. 7. Even though a slight inhibition of cell viability compared to the control was observed following treatment with concentrations of 250 and 500 μg/mL of the samples, the cell viability was still close to 90%. Thus there was a little cytotoxic effect of LMWHs and UFH at high concentrations on A549 cells after incubation for 24 h, while the cytotoxic effect of LMWHs and UFH at low concentrations was negligible.

3.5.2. Scratch wound assay

A549 cell migration was evaluated with a wound healing assay, as shown in Fig. 8a and Fig. 8b. The untreated control group significantly healed after incubation for 48 h. However, both the UFH and LMWH groups reduced the healing ability, which showed that UFH

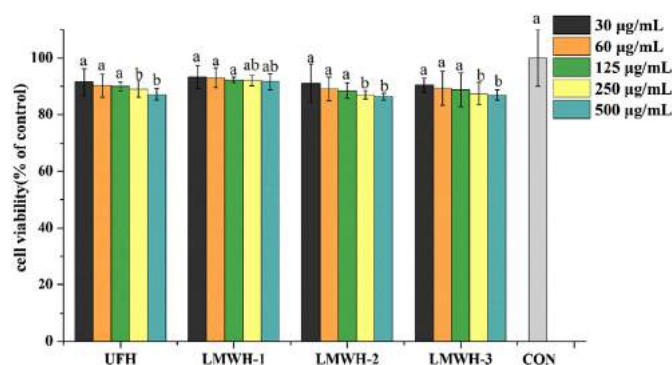


Fig. 7. Effect of UFH and LMWHs on A549 cell viability. A549 cells were seeded into 96-well plates and cultured with different concentrations of UFH and LMWHs (30, 60, 125, 250, 500 μg/mL). Cell viability was evaluated by the MTT assay. Data show the mean ± SD from three independent experiments, $p < 0.05$.

and LMWH exhibited inhibitory effects against cell migration, and the wound healing rates of two different concentrations and two different incubation times are shown in Fig. 8c. Less migration was observed in the LMWH-treated A549 cells, and the wound healing ratio of all samples at a concentration of 500 μg/mL on the migration of A549 cells was found to be lower than that at a concentration of 250 μg/mL. LMWH-3 showed the highest inhibition ratio against A549 cells at $71.44 \pm 4.87\%$ at a concentration of 500 μg/mL, while UFH exhibited moderate inhibition against A549 cells at $24.15 \pm 6.85\%$ when given the same concentration. LMWH—characterized by lower mean molecular weight and a more precisely defined composition of polysaccharidic chains—may have a better efficacy/safety profile [35]. Additionally, the wound healing ratio decreased as the molecular weight of heparin decreased under the same concentration, which may be attributed to the higher uptake rate of oligosaccharides by tumor cells in LMWH compared to UFH [36]. It has also been demonstrated that the anti-growth effect is related to both the size and proportion of different heparin chains. These results were consistent with the findings of several previous studies [24,37,38].

4. Conclusion

The physicochemical depolymerization achieved by combining radical reactions with ultrasonic power can markedly decrease the molecular weight of heparin in a short time. The reaction conditions were kept mild and free of harsh reagents by using H₂O₂ and ascorbic acid to produce free radicals. The products, LMWHs, maintained the major structure of (1 → 4)-linked glucosamine and iduronic acid. The ultrasonic process might make large scale production of LMWH possible, which will be required to expand the scale of application of this system. The LMWHs produced in this study also showed almost no cytotoxicity, and a significant anti-metastasis effect in A549 cells by MTT and scratch wound assay was observed in vitro. LMWH-3 showed the highest inhibition of wound healing in A549 cells. These results suggest the combined method involving radical reactions with ultrasonic power might be suitably used in other sulfated polysaccharide depolymerizations, and the LMWHs produced using this method could be potential therapeutic agents against tumor metastasis. Our future studies will focus on these products' biological activities in vivo.

Acknowledgements

This work was financially supported by National Natural Science Foundation of China (31871815), Key Research and Development

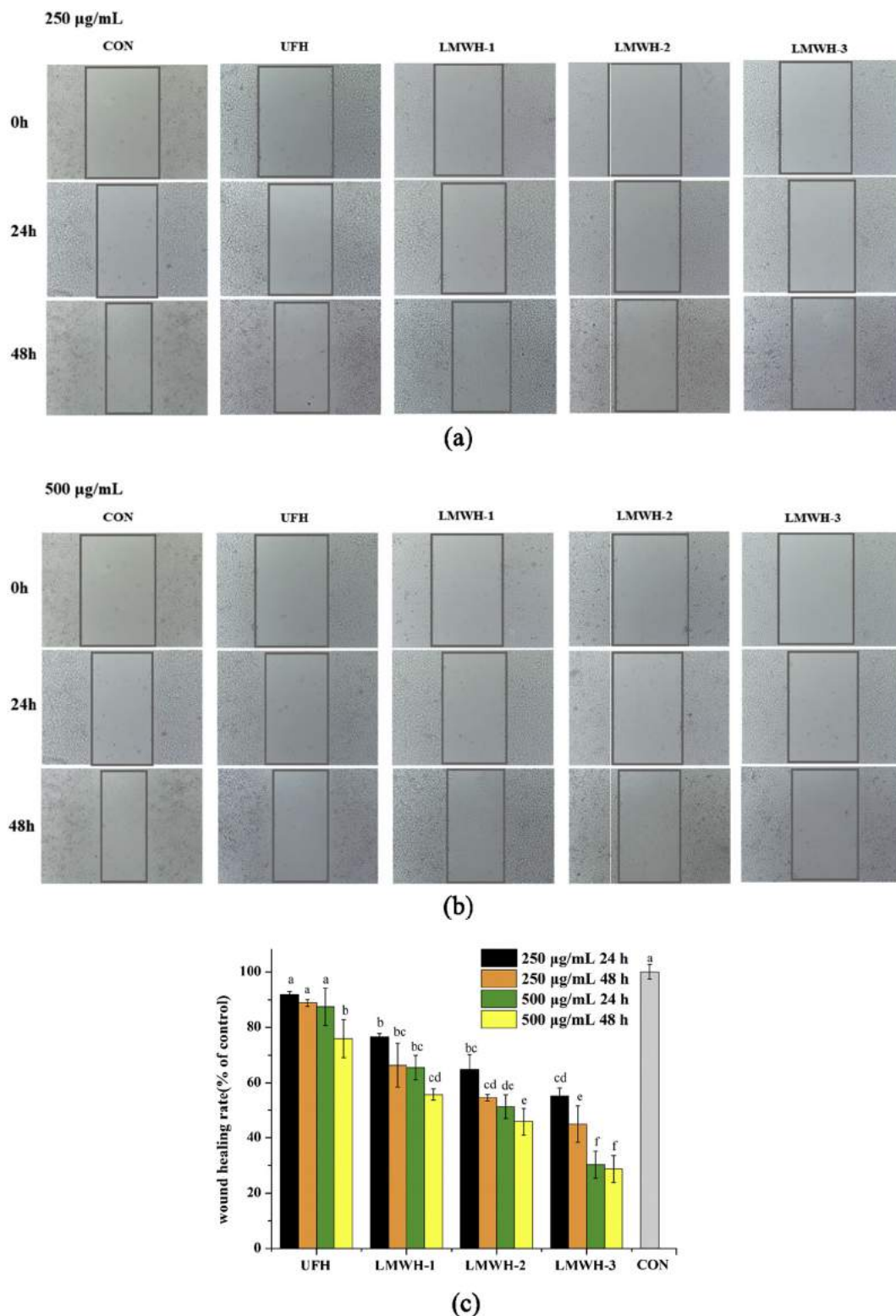


Fig. 8. Representative pictures of the extent of healing when treated with different concentrations of UFH and LMWH for 24 h and 48 h. (a) 250 µg/mL; (b) 500 µg/mL; (c) The rate of wound healing for each group compared to the control (mean ± SD, $n = 3$, $p < 0.05$).

Project of Zhejiang Province, China (2015C02036) and Public Welfare Project of Zhejiang Province, China (2015C32088).

References

- [1] R. Sasisekharan, G. Venkataraman, Heparin and heparan sulfate: biosynthesis, structure and function, *Curr. Opin. Chem. Biol.* 4 (2000) 626–631.
- [2] B. Casu, Structure and biological activity of heparin and other glycosaminoglycans, *Pharmacol. Res. Commun.* 11 (1979) 1–18.
- [3] E.A. Johnson, B. Mulloy, The molecular-weight range of mucosal-heparin preparations, *Carbohydr. Res.* 51 (1976) 119–127.
- [4] J. Harenberg, J.X. de Vries, Characterization of heparins by high-performance size exclusion liquid chromatography, *J. Chromatogr. A* 261 (1983) 287–292.
- [5] M. Petitou, B. Casu, U. Lindahl, 1976–1983, a critical period in the history of heparin: the discovery of the antithrombin binding site, *Biochimie* 85 (2003) 83–89.

- [6] M.D. Freedman, Pharmacodynamics, clinical indications, and adverse effects of heparin, *J. Clin. Pharmacol.* 32 (1992) 584–596.
- [7] M. Monreal, E. Lafoz, R. Salvador, J. Roncales, A. Navarro, Adverse effects of three different forms of heparin therapy: thrombocytopenia, increased transaminases, and hyperkalaemia, *Eur. J. Clin. Pharmacol.* 37 (1989) 415–418.
- [8] J. Hirsh, T.E. Warkentin, S.G. Shaughnessy, S.S. Anand, J.L. Halperin, R. Raschke, C. Granger, E.M. Ohman, J.E. Dalen, Heparin and low-molecular-weight heparin mechanisms of action, pharmacokinetics, dosing, monitoring, efficacy, and safety, *Chest* 119 (2001) 64S–94S.
- [9] R.J. Linhardt, 2003 Claude S. Hudson award address in carbohydrate chemistry. Heparin: structure and activity, *J. Med. Chem.* 46 (2003) 2551–2564.
- [10] R.J. Linhardt, N.S. Gunay, Production and chemical processing of low molecular weight heparins, *Semin. Thromb. Hemost.* (1999) 5–16 (New York: Stratton International Medical Book Corporation).
- [11] K. Nagasawa, H. Uchiyama, N. Sato, A. Hatano, Chemical change involved in the oxidative-reductive depolymerization of heparin, *Carbohydr. Res.* 236 (1992) 165–180.
- [12] K. Rice, Y. Kim, A. Grant, Z. Merchant, R. Linhardt, High-performance liquid chromatographic separation of heparin-derived oligosaccharides, *Anal. Biochem.* 150 (1985) 325–331.
- [13] D. Bergqvist, B. Nilsson, U. Hedner, P. Chr. Pedersen, P.B. Ostergaard, The effect of heparin fragments of different molecular weights on experimental thrombosis and haemostasis, *Thromb. Res.* 38 (1985) 589–601.
- [14] K. Higashi, S. Hosoyama, A. Ohno, S. Masuko, B. Yang, E. Sterner, Z. Wang, R.J. Linhardt, T. Toida, Photochemical preparation of a novel low molecular weight heparin, *Carbohydr. Polym.* 67 (2012) 1737–1743.
- [15] R. Czechowska-Biskup, B. Rokita, S. Lotfy, P. Ulanski, J.M. Rosiak, Degradation of chitosan and starch by 360-kHz ultrasound, *Carbohydr. Polym.* 60 (2005) 175–184.
- [16] C. Zhou, H. Ma, Ultrasonic degradation of polysaccharide from a red algae (*Porphyra yezoensis*), *J. Agric. Food Chem.* 54 (2006) 2223–2228.
- [17] Y. Cheung, J. Yin, J. Wu, Effect of polysaccharide chain conformation on ultrasonic degradation of cudlan in alkaline solution, *Carbohydr. Polym.* 195 (2018) 298–302.
- [18] T. Wu, C. Wu, Y. Xiang, J. Huang, L. Luan, S. Chen, Y. Hu, Kinetics and mechanism of degradation of chitosan by combining sonolysis with H₂O₂/ascorbic acid, *RSC Adv.* 6 (2016) 76280–76287.
- [19] M.F. Zhang, Y.H. Qin, J.Y. Ma, L. Yang, Z.K. Wu, T.L. Wang, W.G. Wang, C.W. Wang, Depolymerization of microcrystalline cellulose by the combination of ultrasound and Fenton reagent, *Ultrason. Sonochem.* 31 (2016) 404–408.
- [20] X. Guo, X. Ye, Y. Sun, D. Wu, N. Wu, Y. Hu, S. Chen, Ultrasound effects on the degradation kinetics, structure, and antioxidant activity of sea cucumber fucoidan, *J. Agric. Food Chem.* 62 (2014) 1088–1095.
- [21] J. Li, S. Li, Z. Zhi, L. Yan, X. Ye, T. Ding, L. Yan, R. Linhardt, S. Chen, Depolymerization of fucosylated chondroitin sulfate with a modified Fenton-system and anticoagulant activity of the resulting fragments, *Mar. Drugs.* 14 (2016) 170.
- [22] M. Wu, S. Xu, J. Zhao, H. Kang, H. Ding, Free-radical depolymerization of glycosaminoglycan from sea cucumber *Thelenata ananas* by hydrogen peroxide and copper ions, *Carbohydr. Polym.* 80 (2010) 1116–1124.
- [23] L. Yan, J. Li, D. Wang, T. Ding, Y. Hu, X. Ye, R.J. Linhardt, S. Chen, Molecular size is important for the safety and selective inhibition of intrinsic factor Xase for fucosylated chondroitin sulfate, *Carbohydr. Polym.* 178 (2017) 180–189.
- [24] C.J. Yu, S.J. Ye, Z.H. Feng, W.J. Ou, X.K. Zhou, L.D. Li, Y.Q. Mao, W. Zhu, Y.Q. Wei, Effect of Fraxiparine, a type of low molecular weight heparin, on the invasion and metastasis of lung adenocarcinoma A549 cells, *Oncol. Lett.* 1 (2010) 755–760.
- [25] C.C. Liang, A.Y. Park, J.L. Guan, In vitro scratch assay: a convenient and inexpensive method for analysis of cell migration in vitro, *Nat. Protoc.* 2 (2007) 329–333.
- [26] O. Achour, N. Bridiau, A. Godhmani, F. Le Joubiou, S. Bordenave Juchereau, F. Sannier, J.M. Piot, I. Fruitier Arnaud, T. Maugard, Ultrasonic-assisted preparation of a low molecular weight heparin (LMWH) with anticoagulant activity, *Carbohydr. Polym.* 97 (2013) 684–689.
- [27] L.J. Bai, J.Y. Wang, The ESR spin trapping studies of reaction between ascorbic acid with hydrogen peroxide, *Chem. J. Chinese. U.* 19 (1998) 890–894.
- [28] G.R. Buettner, B.A. Jurkiewicz, Catalytic metals, ascorbate and free radicals: combinations to avoid, *Radiat. Res.* 145 (1996) 532–541.
- [29] N. Golash, P.R. Gogate, Degradation of dichlorvos containing wastewaters using sonochemical reactors, *Ultrason. Sonochem.* 19 (2012) 1051–1060.
- [30] M. Sivakumar, A.B. Pandit, Ultrasound enhanced degradation of rhodamine B: optimization with power density, *Ultrason. Sonochem.* 8 (2001) 233–240.
- [31] Z. Zhang, J. Xie, H. Liu, J. Liu, R.J. Linhardt, Quantification of heparan sulfate disaccharides using ion-pairing reversed-phase microflow high-performance liquid chromatography with electrospray ionization trap mass spectrometry, *Anal. Chem.* 81 (2009) 4349–4355.
- [32] J. Mao, X. Wang, Q. Li, X. Qi, J. Yang, Preparation and antioxidant properties of low molecular holothurian glycosaminoglycans by H₂O₂/ascorbic acid degradation, *Int. J. Biol. Macromol.* 107 (2018) 1339–1347.
- [33] F. Sun, X. Pang, I. Zhitomirsky, Electrophoretic deposition of composite hydroxyapatite–chitosan–heparin coatings, *J. Mater. Process. Technol.* 209 (2009) 1597–1606.
- [34] T. Yang, A. Hussain, S. Bai, I.A. Khalil, H. Harashima, F. Ahsan, Positively charged polyethylenimines enhance nasal absorption of the negatively charged drug, low molecular weight heparin, *J. Control. Release* 115 (2006) 289–297.
- [35] A. Vignoli, M. Marchetti, L. Russo, E. Cantalino, E. Diani, G. Bonacina, A. Falanga, LMWH bempiparin and ULMWH RO-14 reduce the endothelial angiogenic features elicited by leukemia, lung cancer, or breast cancer cells, *Cancer Investig.* 29 (2011) 153–161.
- [36] P.G. Phillips, M. Yalcin, H. Cui, H. Abdel-Nabi, M. Sajjad, R. Bernacki, J. Veith, S.A. Mousa, Increased tumor uptake of chemotherapeutics and improved chemoresponse by novel non-anticoagulant low molecular weight heparin, *Anticancer Res.* 31 (2011) 411–419.
- [37] A.A. Khorana, A. Sahni, O.D. Altland, C.W. Francis, Heparin inhibition of endothelial cell proliferation and organization is dependent on molecular weight, *Arterioscler. Thromb. Vasc. Biol.* 23 (2003) 2110–2115.
- [38] H. Sun, D. Cao, H. Wu, H. Liu, X. Ke, T. Ci, Development of low molecular weight heparin based nanoparticles for metastatic breast cancer therapy, *Int. J. Biol. Macromol.* 112 (2018) 343–355.